

AperTO - Archivio Istituzionale Open Access dell'Università di Torino

A Conserved Mechanism of APOBEC3 Relocalization by Herpesviral Ribonucleotide Reductase Large Subunits.

This is a pre print version of the following article:

Original Citation:

Availability:

This version is available <http://hdl.handle.net/2318/1726940> since 2020-02-07T14:18:13Z

Published version:

DOI:10.1128/JVI.01539-19

Terms of use:

Open Access

Anyone can freely access the full text of works made available as "Open Access". Works made available under a Creative Commons license can be used according to the terms and conditions of said license. Use of all other works requires consent of the right holder (author or publisher) if not exempted from copyright protection by the applicable law.

(Article begins on next page)

1 **A Conserved Mechanism of APOBEC Counteraction by Herpesviruses**
2 **Ribonucleotide Reductase Large Subunits**

3
4
5 **Running Title: APOBEC Counteraction by Herpesvirus RNRs (54 Char w/ space)**
6
7
8

9 Adam Z. Cheng^{1,2,3,4}, Sofia Nóbrega de Moraes^{1,2,3,4}, Claire Attarian^{1,2,3,4}, Jaime Yockteng-Melgar⁵,
10 Matthew C. Jarvis^{1,2,3,4}, Matteo Biolatti⁶, Ganna Galitska⁶, Valentina Dell'Oste⁶, Lori Frappier⁵, Craig J.
11 Bierle^{3,7}, Stephen A. Rice^{3,8}, & Reuben S. Harris^{1,2,3,4,9,*}
12
13
14

15 ¹ Department of Biochemistry, Molecular Biology and Biophysics, University of Minnesota, Minneapolis,
16 Minnesota, USA, 55455.

17 ² Masonic Cancer Center, University of Minnesota, Minneapolis, Minnesota, USA, 55455.

18 ³ Institute for Molecular Virology, University of Minnesota, Minneapolis, Minnesota, USA, 55455.

19 ⁴ Center for Genome Engineering, University of Minnesota, Minneapolis, Minnesota, USA, 55455.

20 ⁵ Department of Molecular Genetics, University of Toronto, Toronto, Ontario, Canada, M5S 1A8.

21 ⁶ Laboratory of Pathogenesis of Viral Infections, Department of Public Health and Pediatric Sciences,
22 University of Turin, 10126, Turin, Italy

23 ⁷ Department of Pediatrics, Division of Pediatric Infectious Diseases and Immunology, University of
24 Minnesota, Minneapolis, Minnesota, USA 55455

25 ⁸ Department of Microbiology and Immunology, University of Minnesota, Minneapolis, Minnesota, USA,
26 55455.

27 ⁹ Howard Hughes Medical Institute, University of Minnesota, Minneapolis, Minnesota, USA, 55455.

28 * Correspondence: rsh@umn.edu
29

30 **Keywords:** APOBEC3A; APOBEC3B; innate antiviral immunity; herpesviruses; ribonucleotide
31 reductase

32 **Abstract**

33 An integral part of the antiviral innate immune response is the APOBEC3 family of single-stranded DNA
34 cytosine deaminases, which inhibits virus replication through deamination-dependent and -independent
35 activities. Viruses have evolved mechanisms to counteract these enzymes such as HIV-1 Vif-mediated
36 formation of a ubiquitin ligase to degrade virus-restrictive APOBEC3 enzymes. A new example is
37 Epstein-Barr virus (EBV) ribonucleotide reductase (RNR)-mediated inhibition of cellular APOBEC3B
38 (A3B). The large subunit of the viral RNR, BORF2, causes A3B relocalization from the nucleus to
39 cytoplasmic bodies and thereby protects viral DNA during lytic replication. Here, we use
40 co-immunoprecipitation and immunofluorescent microscopy approaches to ask whether this APOBEC
41 neutralization mechanism is shared with the γ -herpesvirus Kaposi's sarcoma-associated herpesvirus
42 (KSHV) and the α -herpesvirus, herpes simplex virus-1 (HSV-1). The large RNR subunit of KSHV,
43 ORF61, co-precipitated multiple APOBEC3s including A3B and APOBEC3A (A3A). KSHV ORF61 also
44 caused relocalization of these two enzymes to perinuclear bodies (A3B) and to oblong cytoplasmic
45 structures (A3A). The large RNR subunit of HSV-1, ICP6, also co-precipitated A3B and A3A and was
46 alone sufficient to promote the relocalization of these enzymes from nuclear to cytoplasmic
47 compartments. HSV-1 infection caused similar relocalization phenotypes, and this was fully dependent on
48 ICP6. These relocalization phenotypes could be exacerbated by infection with viruses that overexpress
49 ICP6 due to an *ICP4* deletion. These results combine to indicate that both γ - and α -herpesviruses
50 counteract the antiviral activities of cellular APOBEC3 enzymes through a similar RNR-dependent
51 mechanism.

52 (236/250)

53

54 **Importance**

55 The APOBEC3 family of DNA cytosine deaminases constitutes a vital innate immune defense against a
56 range of different viruses. A novel counter-restriction mechanism has recently been uncovered for the
57 γ -herpesvirus EBV, in which a subunit of the viral protein known to produce DNA building blocks
58 (ribonucleotide reductase) causes APOBEC3B to relocalize from the nucleus to the cytosol. Here, we
59 extend these observations to a closely related γ -herpesvirus, KSHV, and to a more distantly related
60 α -herpesvirus, HSV-1. Relocalization was also evident for these ribonucleotide reductases and
61 APOBEC3A, which is 92% identical to APOBEC3B. These studies are important because they suggest a
62 conserved mechanism of APOBEC3 evasion by large double-stranded DNA herpesviruses. Strategies to
63 block this host-pathogen interaction may be effective for treating infections by these and other pathogenic
64 herpesviruses.

65 (128/150)

67 **Introduction**

68 There are nine described human herpesviruses (HHV-1 to -8, including HHV6A and 6B), each of
69 which is capable of establishing a lifelong infection [1]. They are among the most prevalent viruses with
70 some such as Epstein-Barr virus (EBV/HHV-4) exceeding 90% seroprevalence in the global population
71 [2]. Primary infection by herpesviruses is often accompanied by mild clinical symptoms and is generally
72 self-limiting before progressing into latency, where the virus persists asymptotically and is capable of
73 periodic cycles of reactivation [3]. A classic example is herpes simplex virus-1 (HSV-1/HHV-1)
74 infection, which produces primary vesicular lesions in the oral mucosa and establishes latency in adjacent
75 neural ganglia where reactivation of the virus leads to formation of repeated lesions in the same area over
76 the course of the infected individual's life [4-6]. Other herpesviruses such as human cytomegalovirus
77 (HCMV/HHV-5) and Kaposi's sarcoma-associated herpesvirus (KSHV/HHV-8) establish latency in
78 various myeloid and lymphoid compartments, often without symptoms associated with reactivation
79 except in the cases of immunosuppression such as organ transplantation or untreated HIV-1 infection [7-
80 13].

81 Overcoming or evading immune surveillance is critical to the survival of human herpesviruses,
82 and these viruses utilize a diverse complement of immunoevasive proteins and RNAs to establish
83 life-long infections [14]. An important arm of the innate immune response lies in the APOBEC family of
84 single-stranded DNA cytosine deaminases [15-17]. Each of the seven APOBEC3 (A3) enzymes, A3A-D
85 and A3F-H, have been implicated in the restriction and hypermutation of a variety of different viruses
86 including lentiviruses (HIV-1, HIV-2, HTLV-1) [18-22], hepadnaviruses (HBV) [23, 24], endogenous
87 retroviruses (LINE-1, Alu) [25, 26], small DNA tumor viruses (HPV, JC/BK-PyV) [27-31], and most
88 recently EBV [32, 33]. It is difficult, if not impossible, to predict *a priori* which subset of APOBEC3
89 enzymes has the potential to engage a given virus and, furthermore, how that virus might counteract
90 potentially restrictive A3 enzymes.

91 Each of the three herpesvirus subfamilies (α , β , and γ) encode both large and small RNR subunits
92 with the exception of β -herpesviruses, which lack a small subunit (**Fig 1A**). These RNRs have the
93 canonical function of synthesizing deoxyribonucleotides by reducing the 2'-hydroxyl from ribonucleotide
94 substrates [34]. While they are essential for all cellular life, the requirement for endogenous viral RNRs
95 differs tremendously across viral families. For example, RNRs are almost ubiquitous among large
96 double-stranded DNA (dsDNA) viruses, such as herpesviruses, poxviruses, and tailed phages
97 (caudovirales), presumably due to high dNTP requirements during DNA replication [35-37]. On the other
98 hand, most small dsDNA viruses and single-stranded DNA viruses do not encode RNRs and instead rely
99 on host-encoded RNRs for deoxyribonucleotide production [38, 39]. In addition to ribonucleotide
100 reductase activity, some viral RNRs have been shown to engage in non-catalytic activities that result in

101 proviral phenotypes. For instance, the HSV-1 and HSV-2 large ribonucleotide reductase subunits, ICP6
102 and ICP10, respectively, have unique N-terminal extensions that block caspase-8 activity to inhibit
103 apoptosis and bind RIP3 to promote necroptosis [40-43] (**Fig 1B**). Interestingly, HCMV UL45 also has
104 anti-apoptotic and pro-necroptotic functions despite lacking a viral small subunit counterpart, suggesting
105 that the primary function of this RNR large subunit is no longer ribonucleotide reduction [43-45].

106 Recently, we identified the ribonucleotide reductase (RNR) large subunit of the γ -herpesvirus
107 EBV as novel inhibitor of APOBEC3B (A3B) [32]. We found that EBV BORF2 functions by directly
108 binding A3B and relocalizing it from the nucleus to the cytoplasmic compartment, which prevents
109 A3B-mediated deamination of cytosines to uracils in viral genomic DNA during lytic replication. In the
110 absence of BORF2, we found that A3B was able to mutate EBV genomes and reduce viral titers and
111 infectivity. We also reported that the homologous protein from KSHV, ORF61, is similarly capable of
112 A3B co-immunoprecipitation and relocalization [32]. Here, we ask whether this novel virus protection
113 mechanism is specific or more general-acting by assessing interactions between γ -herpesvirus
114 BORF2/ORF61 and other human APOBEC3 enzymes and by determining whether the more distantly
115 related α -herpesvirus HSV-1 has a similar A3 neutralization mechanism. We found that, in addition to
116 binding and relocalizing A3B, both BORF2 and ORF61 were also capable of co-immunoprecipitation and
117 relocalization of A3A. More importantly, we found that the HSV-1 RNR large subunit ICP6 similarly
118 binds and relocalizes both A3B and A3A. Overexpression studies showed that ICP6 alone is sufficient for
119 A3B and A3A relocalization. Infection studies with mutants demonstrated that ICP6 is essential and that
120 no other viral protein is capable of this function. These data combined to indicate that pathogenic γ and α -
121 herpesviruses have evolved an effective APOBEC3 counteraction mechanism, which is governed by the
122 viral RNR large subunit.

123

124 **Results**

125 **EBV BORF2 and KSHV ORF61 bind and relocalize both A3B and A3A**

126 Our prior co-immunoprecipitation (co-IP) experiments indicated that EBV BORF2 interacts
127 strongly with A3B and weakly with A3A and A3F (see Fig. 1c in Cheng *et al.* [32]). EBV BORF2 was
128 both necessary and sufficient to relocalize A3B in a variety of different cell types including endogenous
129 A3B in the AGS gastric carcinoma cell line and the M81 B cell line [32]. However, our original studies
130 did not address whether EBV BORF2 could functionally interact with and relocalize any of these related
131 human A3 enzymes. We therefore performed immunofluorescent (IF) microscopy studies of U2OS cells
132 overexpressing A3-mCherry constructs with either empty vector or BORF2-FLAG. As reported, A3B is
133 nuclear, A3A has a cell-wide localization, A3H is cytoplasmic and nucleolar, and the other A3s are
134 cytoplasmic [46-50]. Also as expected, BORF2 caused a robust and complete relocalization of nuclear

135 A3B to perinuclear aggregates (**Fig 2**). Interestingly, BORF2 co-expression with A3A led to the presence
136 of novel linear elongated structures concomitant with normal A3A localization. The localization patterns
137 of the other five A3s were unchanged by BORF2 co-expression. Small BORF2 punctate structures were
138 also noted in all conditions including the mCherry control, which is likely due to transfected BORF2
139 interacting with endogenous A3B (previously shown to be elevated in U2OS [32]). Similar A3B and A3A
140 relocalization patterns were evident in Vero cells except that A3A relocalization became whole-cell
141 without elongated structures (**Supplementary Fig 1**).

142 Like EBV BORF2, KSHV ORF61 was also shown to co-IP and relocalize A3B [32]. However,
143 our original studies did not examine the specificity of this interaction by comparing with related human
144 A3 enzymes. We therefore used co-IP experiments to evaluate KSHV ORF61 interactions with a full
145 panel of human A3 enzymes. ORF61-FLAG was co-expressed with A3-HA family members in 293T
146 cells, subjected to anti-FLAG affinity purification, and analyzed by immunoblotting (**Fig 3A**). The
147 ORF61-FLAG pulldown resulted in A3B recovery as described [32]. However, the ORF61-FLAG IP also
148 yielded a robust interaction with A3A and weaker interactions with A3D and A3F.

149 These KSHV ORF61-A3 interactions were then evaluated by IF microscopy experiments to look
150 for changes in A3 localization in U2OS and Vero cells (**Fig 3B**). As expected [32], KSHV ORF61 caused
151 A3B to relocalize to perinuclear aggregates. Moreover, as above for BORF2 and A3A, ORF61
152 co-expression caused a portion of the cellular A3A to localize to intense elongated linear structures in the
153 cytosolic compartment (**Fig 3B**). No other A3 proteins showed altered subcellular localization in these
154 experiments. These new results with EBV BORF2 and KSHV ORF61 combined to indicate that both
155 A3B and A3A may be cellular targets of viral RNR-mediated neutralization.

156

157 **HSV-1 ICP6 binds and relocalizes A3B and A3A**

158 To test whether RNR-mediated APOBEC antagonism is a more broadly conserved mechanism, a
159 series of co-IP experiments was done with the large RNR subunit of HSV-1, ICP6. FLAG-ICP6 was
160 co-expressed with each of the seven different HA-tagged human A3s in 293T cells and subjected to
161 anti-FLAG IP as above. The EBV BORF2-A3B interaction was used as a positive control and BORF2-
162 A3G as a negative control to be able to compare the relative strengths of pulldowns between RNRs and
163 A3s. HSV-1 ICP6 showed a strong interaction with A3A and weaker, but detectable, interactions with
164 A3B, A3C, and A3D (**Fig 4A**).

165 Next, IF microscopy was used to assess functional interactions between HSV-1 ICP6 and each of
166 the human A3 enzymes. Human U2OS osteosarcoma cells were co-transfected with mCherry-tagged A3s
167 and either empty vector or FLAG-tagged HSV-1 ICP6 and analyzed by IF after 48 hours (**Fig 4B**). On its
168 own EBV BORF2 shows a cytoplasmic distribution and, as shown previously [32], it was able to

169 completely relocalize A3B from the nucleus to cytoplasm. In comparison, HSV-1 FLAG-ICP6 showed a
170 broadly cytoplasmic localization that did not change significantly with co-expression of any A3.
171 However, co-expression of FLAG-ICP6 and A3B-mCherry or A3A-mCherry led to a near complete
172 relocalization of these DNA deaminases from the nucleus to the cytoplasm. HSV-1 ICP6 co-expression
173 with the other A3s did not lead to any remarkable change in localization. These results suggested that,
174 although HSV-1 ICP6 interacted by co-IP with several A3s to varying degrees, functionally relevant
175 interactions may only be occurring with A3B and A3A.

176

177 **HSV-1 infection relocalizes A3B and A3A**

178 To address whether HSV-1 infection similarly promotes relocalization of A3B and A3A, U2OS
179 cells were transfected with A3-mCherry constructs 48 hours prior to either mock or HSV-1 infection. We
180 used K26GFP, a HSV-1 strain that has a GFP moiety fused to capsid protein VP26 to allow for
181 identification of infected cells [51]. Cells were analyzed by IF 8 hours post-infection (hpi) (**Fig 5**). Similar
182 to the ICP6 overexpression experiments described above, HSV-1 infection caused A3A to relocalize to
183 the cytoplasmic compartment and A3B to change from a predominantly nuclear localization to a more
184 cell-wide distribution. A3C also changed from a predominantly cytoplasmic localization to a more diffuse
185 whole cell distribution, whereas A3D, A3F, A3G, and A3H were unchanged by HSV-1 infection. Similar
186 relocalization patterns were found in HeLa cells following HSV-1 K26GFP infection (**Supplementary**
187 **Fig 2**). Moreover, time-course experiments showed that relocalization of A3A was detectable as early as
188 3 hpi, whereas A3B and A3C relocalization became apparent by 6 or 9 hpi (**Supplementary Fig 3**).
189 These kinetic differences may reflect a differential affinity of the viral protein(s) to bind to these cellular
190 A3 enzymes and/or competitions with cellular interactors. Quantification of the mean fluorescence
191 intensity in nuclear and cytoplasmic compartments showed that the nuclear localization of A3A and A3B
192 was significantly decreased upon HSV-1 infection, but A3G localization remained unaltered
193 (**Supplementary Fig 4**).

194

195 **HSV-1-mediated relocalization of A3B and A3A requires ICP6**

196 To investigate whether the HSV-1 large RNR subunit is necessary for A3A/B relocalization, we
197 next examined A3 localization in cells following infection with an HSV-1 KOS1.1 strain lacking ICP6
198 due to a deletion of the *UL39* gene (*UL39* encodes ICP6) [52]. Vero cells were transfected with
199 A3-mCherry constructs 48 hours prior to mock infection or infection with KOS1.1 or KOS1.1ΔICP6.
200 After 8 hours, cells were fixed, permeabilized, and subjected to IF analysis by staining for the HSV-1
201 immediate early protein ICP27 to mark infected cells, and monitoring A3 localization through mCherry
202 fluorescence. As above, HSV-1 infection caused the relocalization of A3A, A3B, and A3C (**Fig 6A**).

203 However, only the relocalization A3A and A3B was ICP6-dependent, whereas A3C redistributed
204 regardless of the presence of ICP6. These results provide strong support for mechanistic conservation of
205 the RNR large subunit-A3 interaction (A3A and A3B) and also indicated that A3C relocalization by
206 HSV-1 is mechanistically distinct.

207 To further investigate the role of ICP6 in mediating A3A and A3B relocalization, U2OS cells
208 were infected with an HSV-1 KOS mutant with a deletion in the *ICP4* gene [53]. ICP4, an immediate
209 early protein, is the major transcriptional activator protein of HSV-1 [53]. *ICP4*-null mutants exhibit a
210 strict block to expression of nearly all viral delayed-early and late genes, but are competent to express the
211 viral immediate-early genes (*ICP0*, *ICP22*, *UL54*, and *US12*) as well the *UL39* gene, a delayed-early gene
212 that is uniquely transactivated by ICP0 [54]. In fact, at intermediate and late times post-infection,
213 *ICP4*-null mutants express abnormally high levels of both the immediate early proteins and ICP6 [53].
214 Similar to what was seen for wild-type HSV-1 infection, infection with the HSV-1 KOS Δ ICP4 mutant
215 also led to A3A and A3B relocalization, but with noticeably more pronounced phenotypes (**Fig 6B**). For
216 instance, this mutant virus caused A3B-mCherry to form perinuclear aggregates reminiscent of previously
217 observed BORF2-A3B bodies [32] (**Fig 6B**). Interestingly, A3C localization remained predominantly
218 nuclear upon HSV-1 KOS Δ ICP4 infection, suggesting that one of the other four immediate early proteins
219 besides ICP4 induces its relocalization. Taken together, these data show that HSV-1 ICP6 is both
220 necessary and sufficient for the relocalization of A3A and A3B, and that at least one other viral factor is
221 responsible for A3C relocalization. Identification of this factor will be the subject of a future
222 investigation.

223

224 Discussion

225 We previously described a novel mechanism of A3B counteraction by γ -herpesvirus RNR large
226 subunits, EBV BORF2 and KSHV ORF61 [32]. These viral proteins interact directly with A3B, relocalize
227 it from the nuclear to the cytoplasmic compartment, and protect lytically replicating viral genomes from
228 A3B-mediated deamination and hypermutation. Here, we investigated the question of specificity by
229 comparing interactions with the full repertoire of seven different human A3 enzymes, and we also
230 addressed the potential for broader conservation by asking whether the α -herpesvirus HSV-1 has a similar
231 APOBEC3 counterdefense mechanism. Although EBV BORF2 and KSHV ORF61 were able to interact
232 with several different A3 proteins in co-IP experiments, these viral RNR large subunits only promoted the
233 relocalization of A3B and A3A. HSV-1 ICP6 showed a similar range of co-IP interactions and also only
234 promoted the relocalization of A3B and A3A. Wild-type but not ICP6 deletion mutant HSV-1 infections
235 yielded similar A3B and A3A relocalization phenotypes. These studies combine to indicate that human γ -
236 and α -herpesviruses possess a conserved A3B/A counterdefense .

237 The question of whether A3B, A3A, or both enzymes are most relevant to herpesvirus
238 pathogenesis is likely to vary among herpesvirus type and depend, at least in part, on the complex
239 interplay between viral tropism(s) and alternating modes of latent versus lytic replication. For EBV,
240 epithelial cells serve as the source of primary infection which are mandatory for establishing lytic
241 replication cycles for person-to-person spread and enabling secondary infection of B lymphocytes for
242 establishment of long-term latency [55]. B cells also support lytic reactivation for reinfection and
243 maintenance of EBV in the blood [56]. Here, A3B may be more important than A3A simply because its
244 expression is well-documented in these cell types [57, 58]. Likewise, KSHV infects epithelial and B cells,
245 but also engages in infection of clinically relevant endothelial cells which can lead to Kaposi's sarcoma
246 [59]. Additionally, monocytes are likely to be a secondary reservoir of latent infection in addition to the B
247 cell reservoir [60-62]. It would therefore not be surprising that KSHV requires the capacity to relocalize
248 both A3B and A3A (A3B neutralization for replication in B cells and A3A neutralization for replication
249 in monocytes/macrophages, where A3A can be expressed at extremely high levels) [57, 63, 64]. For
250 HSV-1, although neither A3B nor A3A expression has been reported in neural/CNS cells, lytic replication
251 in epithelial cells may require functional neutralization of A3B and/or A3A [65, 66]. Of course, dedicated
252 functional studies in the most disease relevant *in vivo* systems will be required to fully address the
253 question of whether A3B, A3A, or both enzymes are most relevant to herpesvirus pathogenesis.

254 Additional studies will also be required to determine if the β -herpesviruses are also able to
255 counteract the activities of APOBEC3 enzymes. Preliminary studies using the HCMV homologue, UL45,
256 showed no detection of interaction with A3B or A3A by co-IP (data not shown), although this alone does
257 not rule-out the absence of an A3 counteraction mechanism. The fact that all herpesviruses analyzed thus
258 far have an ability to relocalize A3B and A3A strongly suggests that these enzymes pose a significant
259 threat to the genetic integrity of these pathogens. Indeed, our prior studies showed that A3B causes
260 declines in both EBV viral titers and infectivity for viruses lacking BORF2. Given the strong mechanistic
261 conservation demonstrated here, we anticipate even larger virus replication phenotypes for RNR mutants
262 in relevant *in vivo* systems. However, such studies will require a structural understanding of the A3-RNR
263 interactions such that separation-of-function mutants can be engineered to dissociate phenotypes due to
264 A3 enzymes and those due to RNR activity as well as other important alternative functions.

265

266 **Materials and Methods**

267 **Generation of herpesvirus phylogenetic tree.** Amino acid sequences for herpesvirus ribonucleotide
268 reductase large subunits were obtained from NCBI Protein RefSeq with the following GenBank accession
269 numbers: HSV-1 ICP6 YP_009137114.1, HSV-2 ICP10 YP_009137191.1, VZV ORF19 NP_040142.1,
270 EBV BORF2 YP_401655.1, HCMV UL45 YP_081503.1, HHV6A U28 NP_042921.1, HHV6B U28

271 NP_050209.1, HHV7 U28 YP_073768.1, KSHV ORF61 YP_001129418.1. Alignment was generated
272 using MUSCLE: multiple sequence alignment with high accuracy and high throughput [67] and
273 phylogenetic tree was made using a neighbor-joining tree without distance corrections. Output was made
274 using FigTree using scaled branches [68].

275 **DNA constructs for expression in human cell lines.** The full set of pcDNA3.1(+) human APOBEC-HA
276 expression constructs has been described [69] [A3A (GenBank accession NM_145699), A3B
277 (NM_004900), A3C (NM_014508), A3D (NM_152426), A3F (NM_145298), A3G (NM021822), A3H
278 (haplotype II; FJ376615)]. The full set of APOBEC-mCherry expression constructs was PCR amplified
279 with Phusion High Fidelity DNA Polymerase (NEB M0530) from previously described A3-mCherry
280 constructs [46] and subcloned into pcDNA5/TO (Invitrogen V103320). The forward PCR primers are as
281 follows: A3A (5'-NNN NAA GCT TAC CAC CAT GGA AGC C-3'), A3B and A3C (5'-NNN NNA
282 AGC TTA CCA CCA TGA ATC CA-3'), A3D (5'-NNN NNA AGC TTA CCA CCA TGA ATC CA-3'),
283 A3F (5'-NNN NNA AGC TTA CCA CCA TGA AGC CT-3'), A3G (5'-NNN NAA GCT TAC CAC
284 CAT GAA GCC T-3'), and A3H (5'-NNN NAA GCT TAC CAC CAT GGC TCT G-3'). The reverse
285 PCR primer used was 5'-AGA GTC GCG GCC GCT TAC TTG TAC A-3'. PCR fragments were
286 digested with *HindIII*-HF (NEB R3104) and *NotI*-HF (NEB R3189) and ligated into pcDNA5/TO. The
287 full set of pLenti-iA3i-HA constructs were previously described except the puromycin resistance gene
288 was replaced with a hygromycin resistance gene [70]. Briefly, this is a lentiviral construct with an intron
289 spanning the A3 gene with a C-terminal 3xHA tag, arranged in the antisense direction, which is expressed
290 after reverse transcription and integration. This construct bypasses limitation of self-restriction by
291 A3-mediated deamination of its own plasmid.

292 EBV BORF2 (GenBank accession V01555.2) with a C-terminal 3x-FLAG (DYKDDDDK) tag
293 and EBV BaRF1 (Genbank accession V01555.2) with a C-terminal 3x-HA (YPYDVPDYA) tag was
294 previously described [32]. Other viral RNRs were subcloned with Phusion High Fidelity DNA
295 Polymerase from previously described pCMV-3F vectors [32].

296 KSHV ORF61 (GenBank accession U75698.1) was PCR amplified using primers 5'-NNN NGA
297 ATT CGC CAC CAT GTC TGT CCG GAC ATT TTG T-3' and 5'-NNN NGA ATT CGC CAC CAT
298 GTC TGT CCG GAC ATT TTG T-3', digested with *EcoRI*-HF (NEB R3101S) and *NotI*-HF, and ligated
299 into pcDNA4 with a C-terminal 3x- FLAG. The same construct was PCR amplified using primers
300 5'-NNN NGC GGC CGC GTC TGT CCG GAC ATT TTG T-3' and 5'-NNN NTC TAG ATT ACT GAC
301 AGA CCA GGC ACT C-3', digested with *NotI*-HF and *XbaI*, and ligated into a similar pcDNA4 vector
302 with N-terminal 3x- FLAG.

303 HSV-1 UL39 (GenBank accession JN555585.1) was PCR amplified using primers 5'-NNN NGA
304 TAT CCG CCA CCA TGG CCA GCC GCC CAG CC-3' and 5'-NNN NGC GGC CGC CCC AGC GCG

305 CAG CT-3', digested with *EcoRV*-HF (NEB R1395) and *NotI*-HF, and ligated into pcDNA4 (Invitrogen
306 V102020) with a C-terminal 3x-FLAG [71]. The same construct was PCR amplified using primers
307 5'-NNN NGC GGC CGC GGC CAG CCG CCC AGC CGC A-3' and 5'-NNN NTC TAG ATT ACA
308 GCG CGC AGC TCG TGC A-3', digested with *NotI*-HF and *XbaI* (NEB R0145S), and ligated into a
309 similar pcDNA4 vector with N-terminal 3x-FLAG.

310 **Human cell culture.** Unless indicated, cell lines were derived from established lab collections. All cell
311 cultures were supplemented with 10% heat-inactivated fetal bovine serum (Gibco 16140-063), 1x
312 Pen-Strep (Thermo Fisher 15140122), and periodically tested for mycoplasma (Lonza MycoAlert PLUS
313 LT07-710). No cell lines have ever been mycoplasma positive or previously treated. 293T and Vero cells
314 were cultured in high glucose DMEM (Hyclone), U2OS cells were cultured in McCoy's 5A media
315 (Hyclone), and HeLa cells were cultured in RPMI 1640 (Corning).

316 **Co-immunoprecipitation experiments and immunoblots.** Semi-confluent 293T cells were grown in
317 6-well plates and transfected with plasmids and 0.6 μ L TransIT-LT1 (Mirus 2304) per 100 ng DNA in
318 100 μ L serum-free Opti-MEM (Thermo Fisher 31985062). A titration series was performed to achieve
319 roughly equivalent protein expression by immunoblot for the A3 panel and RNR homologue co-IP
320 experiments. Growth medium was removed after 48 hrs and whole cells were harvested in 1 mL
321 PBS-EDTA by pipetting. Cells were spun down, PBS-EDTA was removed, and cells were resuspended in
322 300 μ L of ice-cold lysis buffer [150 mM NaCl, 50mM Tris-HCl, 10% glycerol, 1% IGEPAL (Sigma
323 I8896), Roche cOmplete EDTA-free protease inhibitor cocktail tablet (Roche 5056489001), pH 7.4].
324 Cells were vortexed vigorously and left on ice for 30 minutes, then sonicated for 5 seconds in an ice water
325 bath. 30 μ L of whole cell lysate was aliquoted for immunoblot. Lysed cells were spun down at 13,000
326 rpm for 15 minutes to pellet debris and supernatant was added to clean tube with 25 μ L resuspended
327 anti-FLAG M2 Magnetic Beads (Sigma M8823) for overnight incubation at 4 $^{\circ}$ C with gentle rotation.
328 Beads were then washed three times in 700 μ L of ice-cold lysis buffer. Bound protein was eluted in 30 μ L
329 of elution buffer [0.15 mg/mL 3xFLAG peptide (Sigma F4799) in 150 mM NaCl, 50 mM Tris-HCl, 10%
330 glycerol, 0.05% Tergitol, pH 7.4]. Proteins were analyzed by immunoblot and antibodies used include
331 mouse anti-FLAG 1:5000 (Sigma F1804), mouse anti-tubulin 1:10,000 (Sigma T5168), and rabbit
332 anti-HA 1:3000 (Cell Signaling C29F4).

333 **Generation and titration of HSV-1 viruses.** The HSV-1 strains used were wild-type strain KOS1.1 [72],
334 K26GFP [51], ICP6 deletion mutant ICP6 Δ , and the ICP4 deletion mutant d120 [53]. HSV-1 infections
335 were done at a multiplicity of infection of 5 PFU per cell, as previously described [73]. Titers of viral
336 stocks were determined by plaque assay on either Vero cells (KOS1.1, K26GFP, and ICP6 Δ) or
337 ICP4-complementing E5-Vero cells [74].

338 **Immunofluorescence microscopy.** For immunofluorescence imaging of transfected cells, approximately
339 5×10^4 Vero, HeLa, or U2OS cells were plated on coverslips and after 24 hrs, transfected with 200 ng
340 pcDNA4-RNR-3xFLAG, 200 ng pcDNA5/TO-A3-mCherry, or both. After 48 hrs, cells were fixed in 4%
341 formaldehyde, permeabilized in 0.2% Triton X-100 in PBS for 10 minutes, washed three times for 5
342 minutes in PBS, and incubated in blocking buffer (0.0028 M KH_2PO_4 , 0.0072 M K_2HPO_4 , 5% goat serum
343 (Gibco), 5% glycerol, 1% cold water fish gelatin (Sigma), 0.04% sodium azide, pH 7.2) for 1 hr. Cells
344 were then incubated in blocking buffer with primary mouse anti-Flag 1:1000 overnight at 4 °C to detect
345 FLAG-tagged RNRs. Cells were washed 3 times for 5 minutes with PBS, then incubated in secondary
346 antibody goat anti-mouse AlexaFluor 488 1:1000 (Invitrogen A11001) diluted in blocking buffer for 2 hrs
347 at room temperature in the dark. Cells were then counterstained with 1 $\mu\text{g}/\text{mL}$ Hoechst 33342 for 10
348 minutes, rinsed twice for 5 minutes in PBS, and once in sterile water. Coverslips were mounted on
349 pre-cleaned slides (Gold Seal Rite-On) using 20-30 μL of mounting media (dissolve 1g n-propyl gallate
350 (Sigma) in 40 mL glycerol overnight, add 0.35 mL 0.1M KH_2PO_4 , then pH to 8-8.5 with K_2HPO_4 , Q.S. to
351 50mL with water). Slides were imaged on a Nikon Inverted Ti-E Deconvolution Microscope instrument
352 and analyzed using NiS Elements.

353 For immunofluorescence imaging of HSV-1-infected cells, approximately 5×10^4 Vero, HeLa, or
354 U2OS cells were plated on coverslips and after 24 hrs, transfected with 200 ng
355 pcDNA5/TO-A3-mCherry. After 48 hours, cells were infected with HSV-1 K26GFP, HSV-1 KOS1.1,
356 HSV-1 KOS1.1 Δ ICP6, or HSV-1 KOS1.1 Δ ICP4 at MOI 5. Cells were fixed in 4% formaldehyde 8 hours
357 post-infection and then IF studies proceeded as above. Time course experiments were fixed at either 3, 6,
358 9, or 12 hours post-infection. HSV-1 K26GFP experiments did not require primary or secondary antibody
359 staining steps. Cells infected with HSV-1 KOS1.1 and mutants were incubated in primary antibody
360 mouse anti-HSV-1 ICP27 H1113 (Santa Cruz sc69807) 1:1000 overnight at 4 °C to detected
361 HSV-1-infected cells. Secondary antibody staining, counterstaining with Hoechst, mounting, and imaging
362 proceeded as above.

363 For quantification of A3 nuclear to cytoplasmic ratio, IF images were analysed using Fiji
364 software to obtain mean fluorescence intensities (MFI) of nuclear compartments determined by Hoechst
365 stain outline and cytoplasmic compartments determined by cell outline. MFI values were divided and
366 plotted on Prism. Statistical analysis was performed using unpaired Student's t-test.

367

368 **Acknowledgements**

369 We thank Sandy Weller, Neal Deluca, and Prashant Desai for HSV-1 strains, M. Sanders and staff at the
370 University of Minnesota Imaging Center for assistance with fluorescence microscopy, J. Becker for
371 assistance with confocal microscopy, D. Ebrahimi for bioinformatics analyses of A3 expression in

372 different cell types, and P. Southern for thoughtful comments.

373

374 **Author Contributions**

375 Conceptualization, AZC, SAR, and RSH; Investigation, AZC, SNM, and CA; Resources, AZC, CJB, and
376 SAR; Software, MCJ; Supervision, LF, CJB, SAR, and RSH; Validation, AZC, SNM, CA, JY-M, MB,
377 GG, and VDO; Visualization, AZC; Writing – Original Draft, AZC and RSH; Writing – Review &
378 Editing, AZC, SNM, CA, JY-M, MCJ, MB, GG, VDO, LF, CJB, SAR, and RSH.

379

380 **Financial Disclosure Statement**

381 NIH training grants provided salary support for AZC (F30 CA200432 and T32 GM008244) and MCJ
382 (T32 CA009138). JY-M was supported by Secretaría Nacional de Educación Superior, Ciencia,
383 Tecnología e Innovación (SENESCYT). GG is a scholar under the Horizon2020 program (H2020
384 MSCA-ITN-2015). V.D.O. is supported by Research Grants from the University of Turin (RILO18) and
385 from the Italian Ministry of Education, University and Research – MIUR (PRIN 2015, 2015RMNSTA).
386 RSH is the Margaret Harvey Schering Land Grant Chair for Cancer Research, a Distinguished McKnight
387 University Professor, and an Investigator of the Howard Hughes Medical Institute. The funders had no
388 role in study design, data collection and analysis, decision to publish, or preparation of the manuscript.

389

390 **Competing Interests**

391 I have read the journal's policy and the authors of this manuscript have the following competing interest:
392 RSH is a co-founder, shareholder, and consultant of ApoGen Biotechnologies Inc. The other authors have
393 declared that no competing interests exist.

394

395 **Correspondence and requests for materials** should be addressed to RSH (rsh@umn.edu).

396 **References**

- 397 1. Arvin A, Campadelli-Fiume G, Mocarski E, Moore PS, Roizman B, Whitley R, et al. Human
398 Herpesviruses: Biology, Therapy, and Immunoprophylaxis. In: Arvin A, Campadelli-Fiume G,
399 Mocarski E, Moore PS, Roizman B, Whitley R, et al., editors. Human Herpesviruses: Biology,
400 Therapy, and Immunoprophylaxis. Cambridge2007.
- 401 2. Tzellos S, Farrell PJ. Epstein-barr virus sequence variation-biology and disease. *Pathogens*.
402 2012;1(2):156-74.
- 403 3. Grinde B. Herpesviruses: latency and reactivation - viral strategies and host response. *J Oral*
404 *Microbiol*. 2013;5.
- 405 4. Preston CM, Efstathiou S. Molecular basis of HSV latency and reactivation. In: Arvin A,
406 Campadelli-Fiume G, Mocarski E, Moore PS, Roizman B, Whitley R, et al., editors. Human
407 Herpesviruses: Biology, Therapy, and Immunoprophylaxis. Cambridge2007.
- 408 5. Jones C. Herpes simplex virus type 1 and bovine herpesvirus 1 latency. *Clin Microbiol Rev*.
409 2003;16(1):79-95.
- 410 6. Koyuncu OO, MacGibeny MA, Enquist LW. Latent versus productive infection: the alpha
411 herpesvirus switch. *Future Virol*. 2018;13(6):431-43.
- 412 7. Reddehase MJ, Lemmermann NAW. Cellular reservoirs of latent cytomegaloviruses. *Med*
413 *Microbiol Immunol*. 2019.
- 414 8. Aneja KK, Yuan Y. Reactivation and Lytic Replication of Kaposi's Sarcoma-Associated
415 Herpesvirus: An Update. *Front Microbiol*. 2017;8:613.
- 416 9. Cannon MJ, Schmid DS, Hyde TB. Review of cytomegalovirus seroprevalence and demographic
417 characteristics associated with infection. *Rev Med Virol*. 2010;20(4):202-13.
- 418 10. Razonable RR, Humar A, Practice ASTIDCo. Cytomegalovirus in solid organ transplantation.
419 *Am J Transplant*. 2013;13 Suppl 4:93-106.
- 420 11. Ganem D. KSHV infection and the pathogenesis of Kaposi's sarcoma. *Annu Rev Pathol*.
421 2006;1:273-96.

- 422 12. Griffiths P, Baraniak I, Reeves M. The pathogenesis of human cytomegalovirus. *J Pathol.*
423 2015;235(2):288-97.
- 424 13. Britt W. Virus entry into host, establishment of infection, spread in host, mechanisms of tissue
425 damage. In: Arvin A, Campadelli-Fiume G, Mocarski E, Moore PS, Roizman B, Whitley R, et al.,
426 editors. *Human Herpesviruses: Biology, Therapy, and Immunoprophylaxis.* Cambridge 2007.
- 427 14. Paludan SR, Bowie AG, Horan KA, Fitzgerald KA. Recognition of herpesviruses by the innate
428 immune system. *Nat Rev Immunol.* 2011;11(2):143-54.
- 429 15. Simon V, Bloch N, Landau NR. Intrinsic host restrictions to HIV-1 and mechanisms of viral
430 escape. *Nat Immunol.* 2015;16(6):546-53.
- 431 16. Harris RS, Dudley JP. APOBECs and virus restriction. *Virology.* 2015;479-480:131-45.
- 432 17. Malim MH, Emerman M. HIV-1 accessory proteins--ensuring viral survival in a hostile
433 environment. *Cell Host Microbe.* 2008;3(6):388-98.
- 434 18. Sheehy AM, Gaddis NC, Choi JD, Malim MH. Isolation of a human gene that inhibits HIV-1
435 infection and is suppressed by the viral Vif protein. *Nature.* 2002;418(6898):646-50.
- 436 19. Harris RS, Bishop KN, Sheehy AM, Craig HM, Petersen-Mahrt SK, Watt IN, et al. DNA
437 deamination mediates innate immunity to retroviral infection. *Cell.* 2003;113(6):803-9.
- 438 20. Wiegand HL, Doehle BP, Bogerd HP, Cullen BR. A second human antiretroviral factor,
439 APOBEC3F, is suppressed by the HIV-1 and HIV-2 Vif proteins. *EMBO J.* 2004;23(12):2451-8.
- 440 21. Sasada A, Takaori-Kondo A, Shirakawa K, Kobayashi M, Abudu A, Hishizawa M, et al.
441 APOBEC3G targets human T-cell leukemia virus type 1. *Retrovirology.* 2005;2:32.
- 442 22. Dang Y, Wang X, Esselman WJ, Zheng YH. Identification of APOBEC3DE as another
443 antiretroviral factor from the human APOBEC family. *J Virol.* 2006;80(21):10522-33.
- 444 23. Turelli P, Mangeat B, Jost S, Vianin S, Trono D. Inhibition of hepatitis B virus replication by
445 APOBEC3G. *Science.* 2004;303(5665):1829.

- 446 24. Suspene R, Guetard D, Henry M, Sommer P, Wain-Hobson S, Vartanian JP. Extensive editing of
447 both hepatitis B virus DNA strands by APOBEC3 cytidine deaminases in vitro and in vivo. Proc
448 Natl Acad Sci U S A. 2005;102(23):8321-6.
- 449 25. Esnault C, Heidmann O, Delebecque F, Dewannieux M, Ribet D, Hance AJ, et al. APOBEC3G
450 cytidine deaminase inhibits retrotransposition of endogenous retroviruses. Nature.
451 2005;433(7024):430-3.
- 452 26. Chiu YL, Witkowska HE, Hall SC, Santiago M, Soros VB, Esnault C, et al. High-molecular-mass
453 APOBEC3G complexes restrict Alu retrotransposition. Proc Natl Acad Sci U S A.
454 2006;103(42):15588-93.
- 455 27. Vieira VC, Leonard B, White EA, Starrett GJ, Temiz NA, Lorenz LD, et al. Human
456 papillomavirus E6 triggers upregulation of the antiviral and cancer genomic DNA deaminase
457 APOBEC3B. MBio. 2014;5(6).
- 458 28. Vartanian JP, Guetard D, Henry M, Wain-Hobson S. Evidence for editing of human
459 papillomavirus DNA by APOBEC3 in benign and precancerous lesions. Science.
460 2008;320(5873):230-3.
- 461 29. Peretti A, Geoghegan EM, Pastrana DV, Smola S, Feld P, Sauter M, et al. Characterization of BK
462 Polyomaviruses from Kidney Transplant Recipients Suggests a Role for APOBEC3 in Driving
463 In-Host Virus Evolution. Cell Host Microbe. 2018;23(5):628-35 e7.
- 464 30. Verhalen B, Starrett GJ, Harris RS, Jiang M. Functional Upregulation of the DNA Cytosine
465 Deaminase APOBEC3B by Polyomaviruses. J Virol. 2016;90(14):6379-86.
- 466 31. Narvaiza I, Linfesty DC, Greener BN, Hakata Y, Pintel DJ, Logue E, et al. Deaminase-
467 independent inhibition of parvoviruses by the APOBEC3A cytidine deaminase. PLoS Pathog.
468 2009;5(5):e1000439.
- 469 32. Cheng AZ, Yockteng-Melgar J, Jarvis MC, Malik-Soni N, Borozan I, Carpenter MA, et al.
470 Epstein-Barr virus BORF2 inhibits cellular APOBEC3B to preserve viral genome integrity. Nat
471 Microbiol. 2019;4(1):78-88.

- 472 33. Martinez T, Shapiro M, Bhaduri-McIntosh S, MacCarthy T. Evolutionary effects of the
473 AID/APOBEC family of mutagenic enzymes on human gamma-herpesviruses. *Virus Evol.*
474 2019;5(1):vey040.
- 475 34. Torrents E. Ribonucleotide reductases: essential enzymes for bacterial life. *Front Cell Infect*
476 *Microbiol.* 2014;4:52.
- 477 35. Iyer LM, Aravind L, Koonin EV. Common origin of four diverse families of large eukaryotic
478 DNA viruses. *J Virol.* 2001;75(23):11720-34.
- 479 36. Sakowski EG, Munsell EV, Hyatt M, Kress W, Williamson SJ, Nasko DJ, et al. Ribonucleotide
480 reductases reveal novel viral diversity and predict biological and ecological features of unknown
481 marine viruses. *Proc Natl Acad Sci U S A.* 2014;111(44):15786-91.
- 482 37. Zhao Y, Temperton B, Thrash JC, Schwalbach MS, Vergin KL, Landry ZC, et al. Abundant
483 SAR11 viruses in the ocean. *Nature.* 2013;494(7437):357-60.
- 484 38. Cohen D, Adamovich Y, Reuven N, Shaul Y. Hepatitis B virus activates deoxynucleotide
485 synthesis in nondividing hepatocytes by targeting the R2 gene. *Hepatology.* 2010;51(5):1538-46.
- 486 39. Kitab B, Satoh M, Ohmori Y, Munakata T, Sudoh M, Kohara M, et al. Ribonucleotide reductase
487 M2 promotes RNA replication of hepatitis C virus by protecting NS5B protein from hPLIC1-
488 dependent proteasomal degradation. *J Biol Chem.* 2019;294(15):5759-73.
- 489 40. Langelier Y, Bergeron S, Chabaud S, Lippens J, Guilbault C, Sasseville AM, et al. The R1
490 subunit of herpes simplex virus ribonucleotide reductase protects cells against apoptosis at, or
491 upstream of, caspase-8 activation. *J Gen Virol.* 2002;83(Pt 11):2779-89.
- 492 41. Dufour F, Sasseville AM, Chabaud S, Massie B, Siegel RM, Langelier Y. The ribonucleotide
493 reductase R1 subunits of herpes simplex virus types 1 and 2 protect cells against TNFalpha- and
494 FasL-induced apoptosis by interacting with caspase-8. *Apoptosis.* 2011;16(3):256-71.
- 495 42. Huang Z, Wu SQ, Liang Y, Zhou X, Chen W, Li L, et al. RIP1/RIP3 binding to HSV-1 ICP6
496 initiates necroptosis to restrict virus propagation in mice. *Cell Host Microbe.* 2015;17(2):229-42.

- 497 43. Mocarski ES, Guo H, Kaiser WJ. Necroptosis: The Trojan horse in cell autonomous antiviral host
498 defense. *Virology*. 2015;479-480:160-6.
- 499 44. Kwon KM, Oh SE, Kim YE, Han TH, Ahn JH. Cooperative inhibition of RIP1-mediated NF-
500 kappaB signaling by cytomegalovirus-encoded deubiquitinase and inactive homolog of cellular
501 ribonucleotide reductase large subunit. *PLoS Pathog*. 2017;13(6):e1006423.
- 502 45. Mack C, Sickmann A, Lembo D, Brune W. Inhibition of proinflammatory and innate immune
503 signaling pathways by a cytomegalovirus RIP1-interacting protein. *Proc Natl Acad Sci U S A*.
504 2008;105(8):3094-9.
- 505 46. Lackey L, Law EK, Brown WL, Harris RS. Subcellular localization of the APOBEC3 proteins
506 during mitosis and implications for genomic DNA deamination. *Cell Cycle*. 2013;12(5):762-72.
- 507 47. Salamango DJ, McCann JL, Demir O, Brown WL, Amaro RE, Harris RS. APOBEC3B Nuclear
508 Localization Requires Two Distinct N-Terminal Domain Surfaces. *J Mol Biol*.
509 2018;430(17):2695-708.
- 510 48. Salamango DJ, Becker JT, McCann JL, Cheng AZ, Demir O, Amaro RE, et al. APOBEC3H
511 Subcellular Localization Determinants Define Zipcode for Targeting HIV-1 for Restriction. *Mol*
512 *Cell Biol*. 2018;38(23).
- 513 49. Muckenfuss H, Hamdorf M, Held U, Perkovic M, Lower J, Cichutek K, et al. APOBEC3 proteins
514 inhibit human LINE-1 retrotransposition. *J Biol Chem*. 2006;281(31):22161-72.
- 515 50. Bogerd HP, Wiegand HL, Hulme AE, Garcia-Perez JL, O'Shea KS, Moran JV, et al. Cellular
516 inhibitors of long interspersed element 1 and Alu retrotransposition. *Proc Natl Acad Sci U S A*.
517 2006;103(23):8780-5.
- 518 51. Desai P, Person S. Incorporation of the green fluorescent protein into the herpes simplex virus
519 type 1 capsid. *J Virol*. 1998;72(9):7563-8.
- 520 52. Goldstein DJ, Weller SK. Factor(s) present in herpes simplex virus type 1-infected cells can
521 compensate for the loss of the large subunit of the viral ribonucleotide reductase: characterization
522 of an ICP6 deletion mutant. *Virology*. 1988;166(1):41-51.

- 523 53. DeLuca NA, McCarthy AM, Schaffer PA. Isolation and characterization of deletion mutants of
524 herpes simplex virus type 1 in the gene encoding immediate-early regulatory protein ICP4. *J*
525 *Virology*. 1985;56(2):558-70.
- 526 54. Desai P, Ramakrishnan R, Lin ZW, Osak B, Glorioso JC, Levine M. The RR1 gene of herpes
527 simplex virus type 1 is uniquely trans activated by ICP0 during infection. *J Virology*.
528 1993;67(10):6125-35.
- 529 55. Sitki-Green D, Covington M, Raab-Traub N. Compartmentalization and transmission of multiple
530 Epstein-Barr virus strains in asymptomatic carriers. *J Virology*. 2003;77(3):1840-7.
- 531 56. Kenney SC, Mertz JE. Regulation of the latent-lytic switch in Epstein-Barr virus. *Semin Cancer*
532 *Biology*. 2014;26:60-8.
- 533 57. Koning FA, Newman EN, Kim EY, Kunstman KJ, Wolinsky SM, Malim MH. Defining
534 APOBEC3 expression patterns in human tissues and hematopoietic cell subsets. *J Virology*.
535 2009;83(18):9474-85.
- 536 58. Burns MB, Lackey L, Carpenter MA, Rathore A, Land AM, Leonard B, et al. APOBEC3B is an
537 enzymatic source of mutation in breast cancer. *Nature*. 2013;494(7437):366-70.
- 538 59. Chakraborty S, Veetil MV, Chandran B. Kaposi's Sarcoma Associated Herpesvirus Entry into
539 Target Cells. *Front Microbiology*. 2012;3:6.
- 540 60. Blasig C, Zietz C, Haar B, Neipel F, Esser S, Brockmeyer NH, et al. Monocytes in Kaposi's
541 sarcoma lesions are productively infected by human herpesvirus 8. *J Virology*. 1997;71(10):7963-8.
- 542 61. Wu W, Vieira J, Fiore N, Banerjee P, Sieburg M, Rochford R, et al. KSHV/HHV-8 infection of
543 human hematopoietic progenitor (CD34+) cells: persistence of infection during hematopoiesis in
544 vitro and in vivo. *Blood*. 2006;108(1):141-51.
- 545 62. Kim IJ, Flano E, Woodland DL, Lund FE, Randall TD, Blackman MA. Maintenance of long term
546 gamma-herpesvirus B cell latency is dependent on CD40-mediated development of memory B
547 cells. *J Immunology*. 2003;171(2):886-92.

- 548 63. Stenglein MD, Burns MB, Li M, Lengyel J, Harris RS. APOBEC3 proteins mediate the clearance
549 of foreign DNA from human cells. *Nat Struct Mol Biol.* 2010;17(2):222-9.
- 550 64. Thielen BK, McNevin JP, McElrath MJ, Hunt BV, Klein KC, Lingappa JR. Innate immune
551 signaling induces high levels of TC-specific deaminase activity in primary monocyte-derived
552 cells through expression of APOBEC3A isoforms. *J Biol Chem.* 2010;285(36):27753-66.
- 553 65. Nicoll MP, Proenca JT, Efstathiou S. The molecular basis of herpes simplex virus latency.
554 2012;36(3):684-705.
- 555 66. Akhtar J, Shukla D. Viral entry mechanisms: cellular and viral mediators of herpes simplex virus
556 entry. *FEBS J.* 2009;276(24):7228-36.
- 557 67. Edgar RC. MUSCLE: multiple sequence alignment with high accuracy and high throughput.
558 *Nucleic Acids Res.* 2004;32(5):1792-7.
- 559 68. Bouckaert R, Heled J, Kuhnert D, Vaughan T, Wu CH, Xie D, et al. BEAST 2: a software
560 platform for Bayesian evolutionary analysis. *PLoS Comput Biol.* 2014;10(4):e1003537.
- 561 69. Larue RS, Lengyel J, Jonsson SR, Andresdottir V, Harris RS. Lentiviral Vif degrades the
562 APOBEC3Z3/APOBEC3H protein of its mammalian host and is capable of cross-species activity.
563 *J Virol.* 2010;84(16):8193-201.
- 564 70. Law EK, Sieuwerts AM, LaPara K, Leonard B, Starrett GJ, Molan AM, et al. The DNA cytosine
565 deaminase APOBEC3B promotes tamoxifen resistance in ER-positive breast cancer. *Sci Adv.*
566 2016;2(10):e1601737.
- 567 71. Jager S, Kim DY, Hultquist JF, Shindo K, LaRue RS, Kwon E, et al. Vif hijacks CBF-beta to
568 degrade APOBEC3G and promote HIV-1 infection. *Nature.* 2011;481(7381):371-5.
- 569 72. Hughes RG, Jr., Munyon WH. Temperature-sensitive mutants of herpes simplex virus type 1
570 defective in lysis but not in transformation. *J Virol.* 1975;16(2):275-83.
- 571 73. Park D, Lalli J, Sedlackova-Slavikova L, Rice SA. Functional comparison of herpes simplex
572 virus 1 (HSV-1) and HSV-2 ICP27 homologs reveals a role for ICP27 in virion release. *J Virol.*
573 2015;89(5):2892-905.

574 74. DeLuca NA, Schaffer PA. Physical and functional domains of the herpes simplex virus
575 transcriptional regulatory protein ICP4. J Virol. 1988;62(3):732-43.

576

577 **Figure Legends**

578

579 **Fig 1. Herpesvirus ribonucleotide reductases conservation.**

580 (A) Amino acid sequences from ribonucleotide reductase large subunits were aligned using Multiple
581 Sequence Comparison by Log-Expectation (MUSCLE) and phylogeny was constructed using
582 neighbor-joining tree without distance corrections and scaled for equal branch lengths (scale bar = 1).
583 Shaded boxes indicate herpesvirus subfamilies, which group closely to established phylogenetic trees.
584 Protein names for human herpesvirus ribonucleotide reductase large and small subunits shown on the
585 right.

586 (B) Schematic of representative RNR large subunit polypeptides from α -, β -, and γ -herpesviruses with
587 conserved core sequences (colored) and unique N- and C-terminal extensions (gray). Diagram is
588 approximately to scale with a ~190 amino acid portion of HSV-1 ICP6 omitted to fit the figure. Scale bar
589 is 100 amino acids.

590

591 **Fig 2. EBV BORF2 relocates A3B and A3A.**

592 Representative images of U2OS cells transfected with either A3-mCherry or BORF2-FLAG constructs.
593 Cells were fixed 48 hours post-transfection, permeabilized, and stained with anti-FLAG antibody and
594 Hoechst. A3 localization was compared in the presence and absence of EBV BORF2-FLAG
595 co-transfection.

596

597 **Fig 3. KSHV ORF61 relocates A3B and A3A.**

598 (A) Co-immunoprecipitation of transfected KSHV ORF61-FLAG with the indicated A3-HA constructs in
599 293T cells. Cells were lysed 48 hours post-transfection for anti-FLAG pulldown and resulting proteins
600 were analyzed by immunoblot. EBV FLAG-BORF2 transfected with A3B and A3G were used as positive
601 and negative co-IP controls, respectively.

602 (B) Representative images of U2OS cells transfected with either A3-mCherry or FLAG-RNR constructs.
603 Cells were fixed 48 hours post-transfection, permeabilized, and stained with anti-FLAG antibody and
604 Hoechst. Co-transfection with A3B-mCherry and EBV BORF2-FLAG was used as positive controls for
605 relocalization from nuclear to cytoplasmic aggregates. A3 localization was compared in the presence and
606 absence of KSHV ORF61-FLAG co-transfection.

607

608 **Fig 4. HSV-1 ICP6 binds and relocates A3B and A3A.**

609 (A) Co-immunoprecipitation of transfected HSV-1 FLAG-ICP6 with the indicated A3-HA constructs in
610 293T cells. Cells were lysed 48 hours post-transfection for anti-FLAG pulldown and resulting proteins

611 were analyzed by immunoblot. EBV FLAG-BORF2 transfected with A3B and A3G were used as positive
612 and negative co-IP controls, respectively.

613 **(B)** Representative images of U2OS cells transfected with either A3-mCherry or FLAG-RNR constructs.
614 Cells were fixed 48 hours post-transfection, permeabilized, and stained with anti-FLAG antibody and
615 Hoechst. Co-transfection with A3B-mCherry and EBV FLAG-BORF2 was used as positive controls for
616 relocalization from nuclear to cytoplasmic aggregates. A3 localization was compared in the presence and
617 absence of HSV-1 FLAG- ICP6 co-transfection.

618

619 **Fig 5. HSV-1 infection relocalizes A3B and A3A.**

620 Representative images of U2OS cells transfected with A3-mCherry constructs, followed by mock or
621 HSV-1 K26GFP infection 48 hours post-transfection. Cells were fixed 8 hpi and stained with Hoechst,
622 then imaged directly. The viral capsid protein VP26 is tagged with GFP which marks infected cells.

623

624 **Fig 6. A3B and A3A relocalization is dependent on HSV-1 ICP6.**

625 **(A)** Representative images of Vero cells transfected with A3-mCherry constructs, followed by mock,
626 wild-type HSV-1 KOS1.1, or HSV-1 KOS1.1 Δ ICP6 infection 48 hours post-transfection. Cells were
627 fixed 8 hours after HSV-1 infection, permeabilized, and stained with anti-ICP27 antibody to mark
628 infected cells and Hoechst.

629 **(B)** Representative images from an experiment similar to that described in panel A, except using U2OS
630 cells and the mutant virus HSV-1 KOS1.1 Δ ICP4.

631

632

633

634 **Supporting Information**

635 **Supplementary Fig 1. EBV BORF2 relocalizes A3B and A3A.**

636 Representative immunofluorescence microscopy images of Vero cells transfected with either A3-mCherry
637 or EBV BORF2-FLAG constructs. Cells were fixed 48 hours post-transfection, permeabilized, and
638 stained with anti-FLAG antibody and Hoechst to stain the nuclear compartment.

639

640 **Supplementary Fig 2. HSV-1 infection relocalizes A3B and A3A.**

641 Representative images of Vero cells transfected with A3-mCherry constructs, followed by mock or
642 HSV-1 K26GFP infection 48 hours post-transfection. Cells were fixed 8 hpi and then imaged directly.
643 The viral capsid protein VP26 is tagged with GFP to mark infected cells.

644

645 **Supplementary Fig 3. Time course of HSV-1-mediated relocalization of A3B and A3A.**

646 Representative images of U2OS cells transfected with A3-mCherry constructs, followed by mock or
647 HSV-1 KOS1.1 infection 48 hours post-transfection. Cells were fixed at either 3, 6, 9, or 12 hpi and
648 stained with anti-ICP27 antibody to mark infected cells and Hoechst to stain the nuclear compartment.

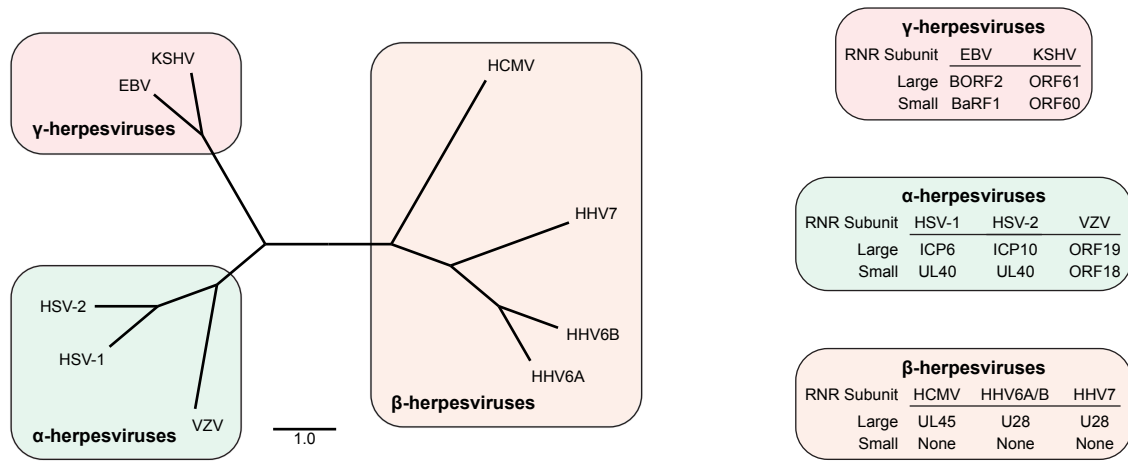
649

650 **Supplementary Fig 4. A3B and A3A localization is altered by HSV-1 infection.**

651 Quantification of A3 localization patterns with or without HSV-1 infection by dividing the mean
652 fluorescence intensity of the nuclear and cytoplasmic compartments. Data points are pooled evenly from
653 immunofluorescence microscopy images shown in Figs. 5 and 6. Statistical analysis was performed using
654 an unpaired Student's t-test between indicated groups, NS = not significant).

655

Fig 1
A



B

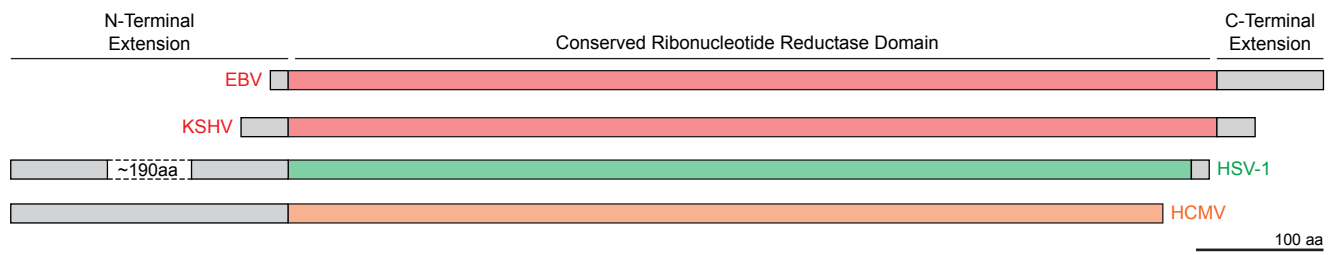


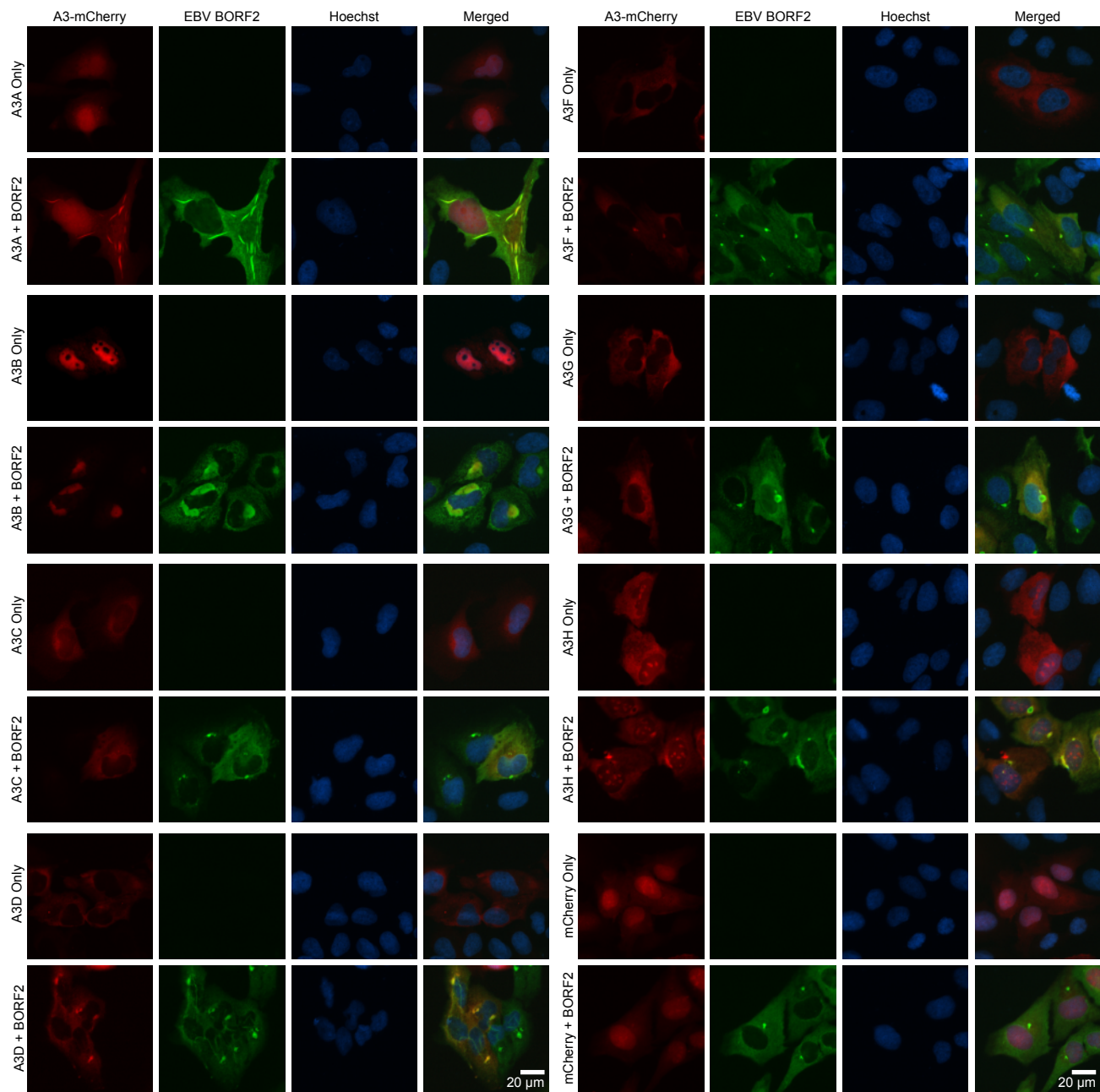
Fig 2

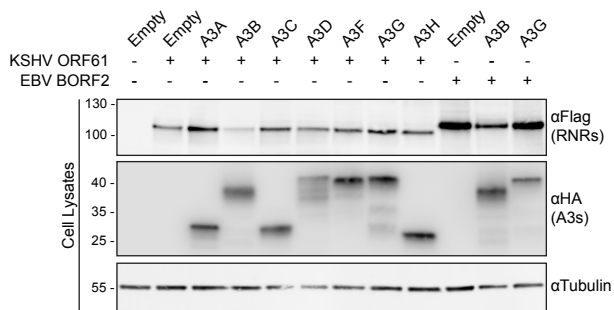
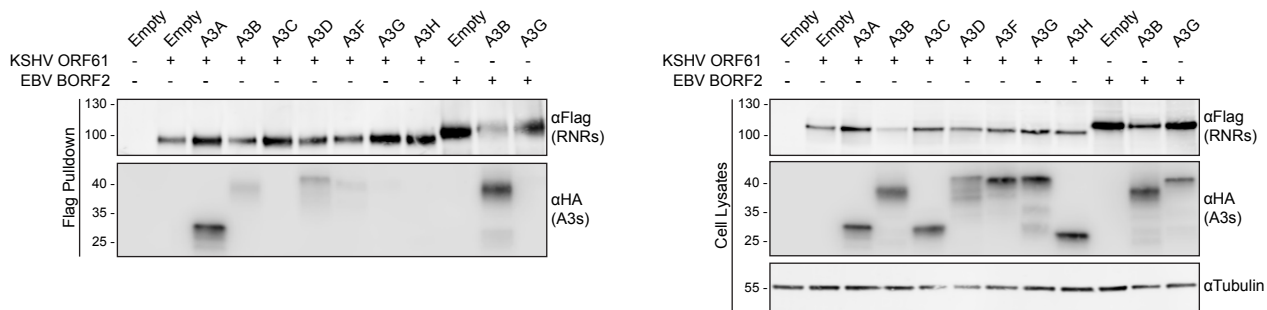
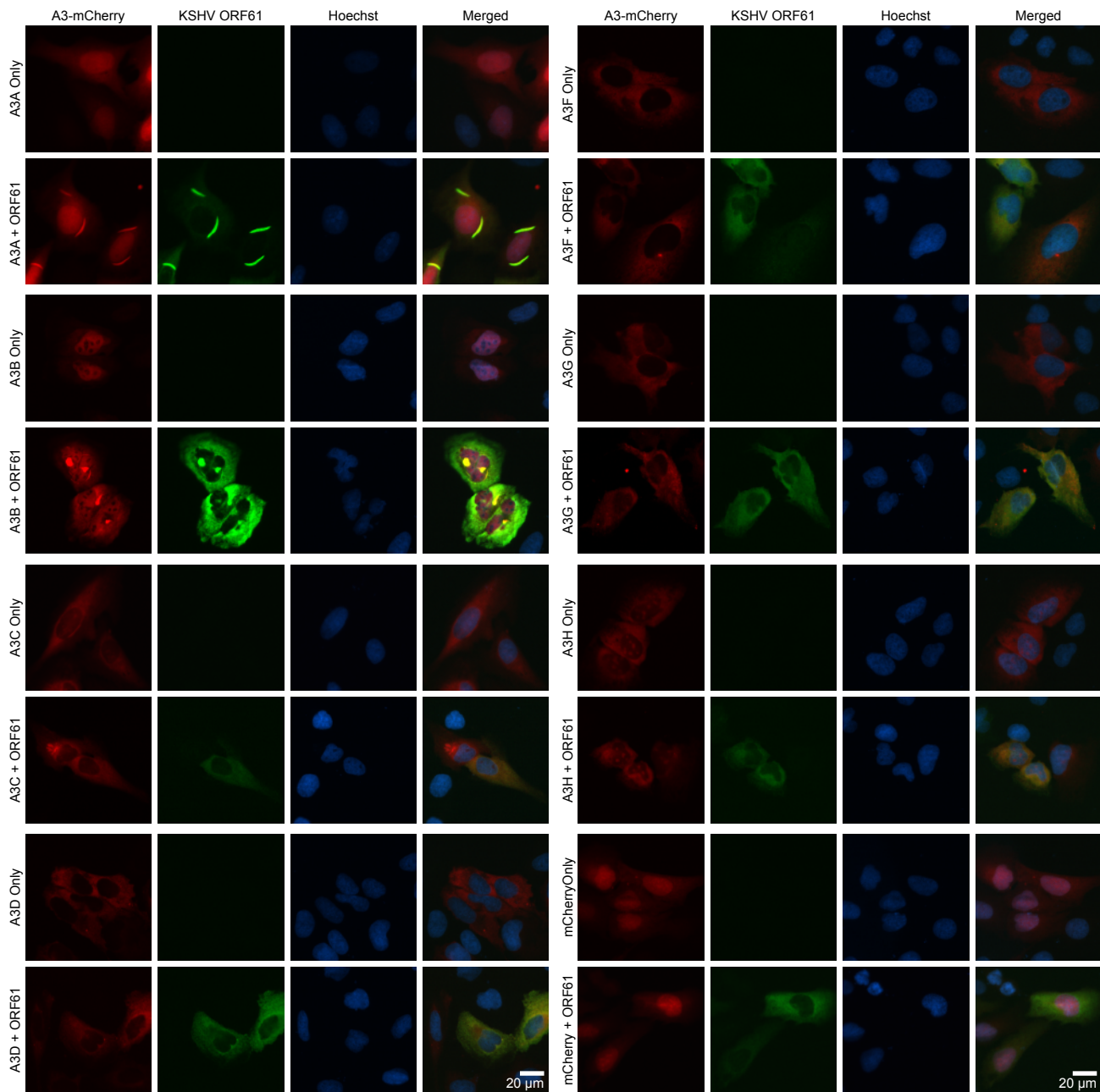
Fig 3**A****B**

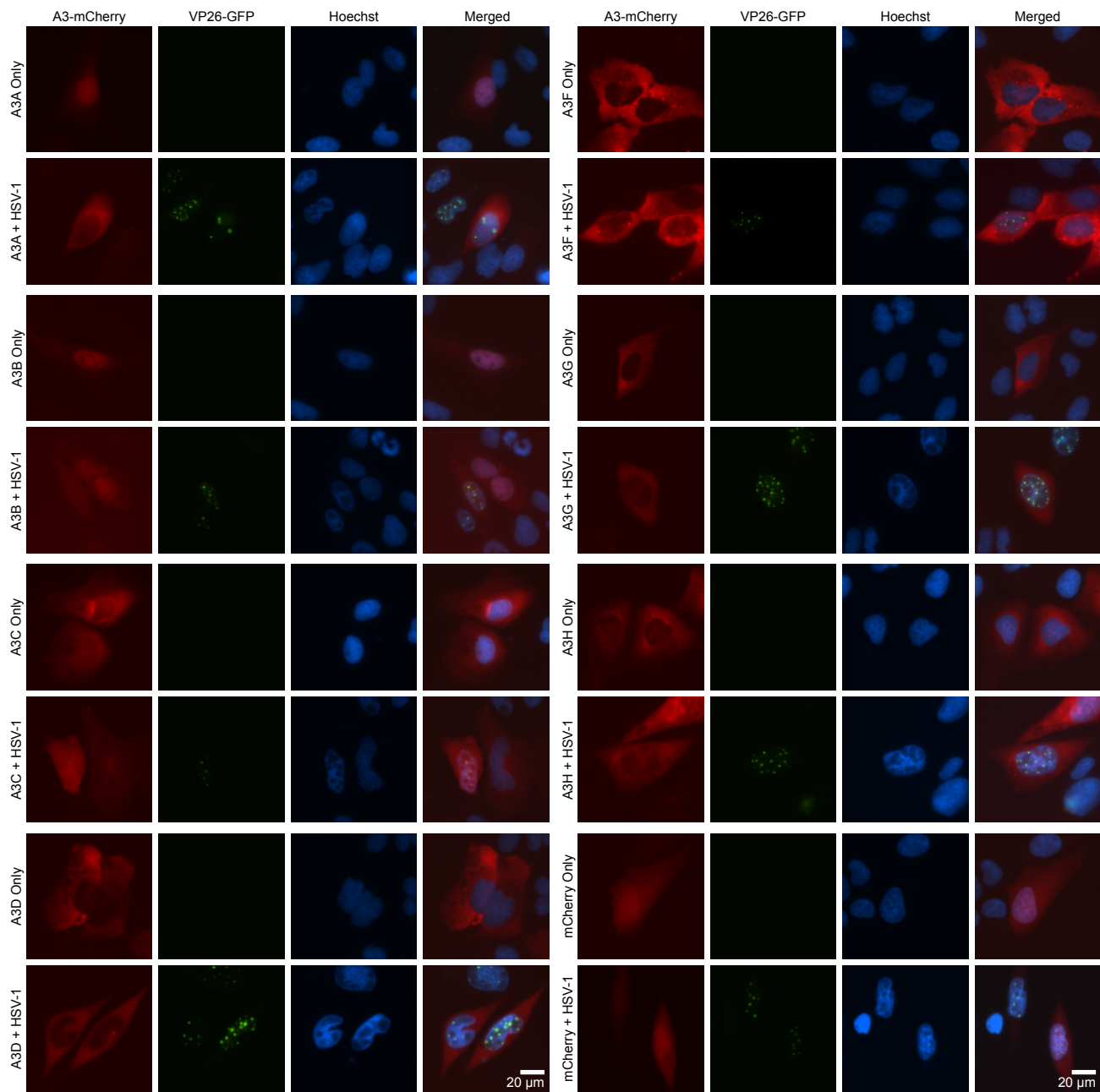
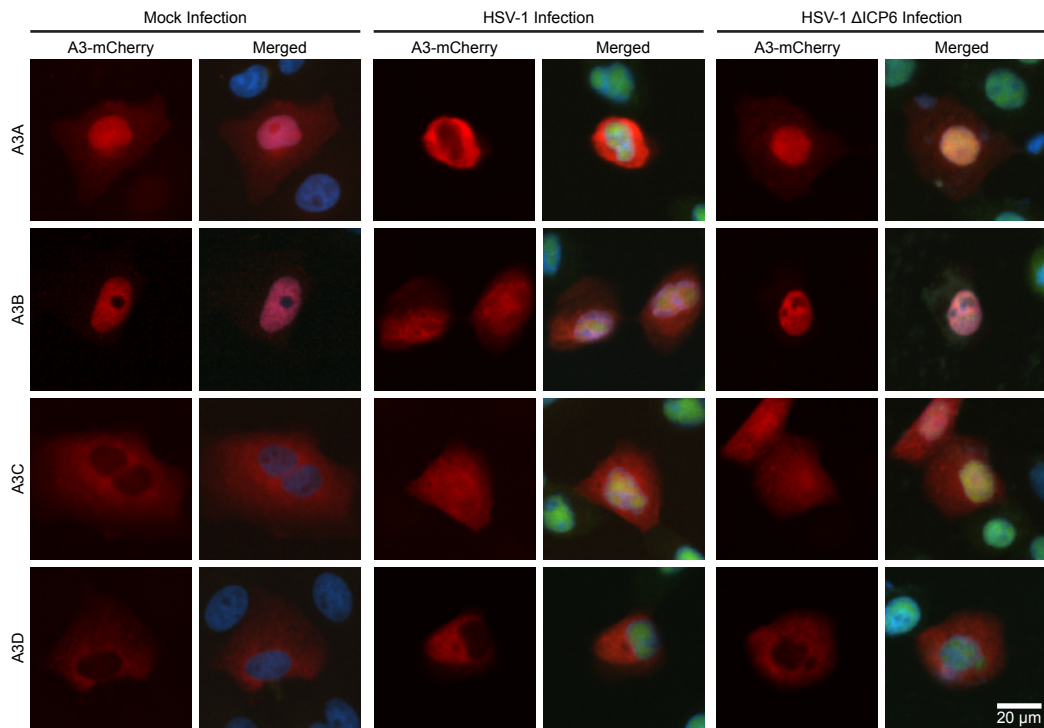
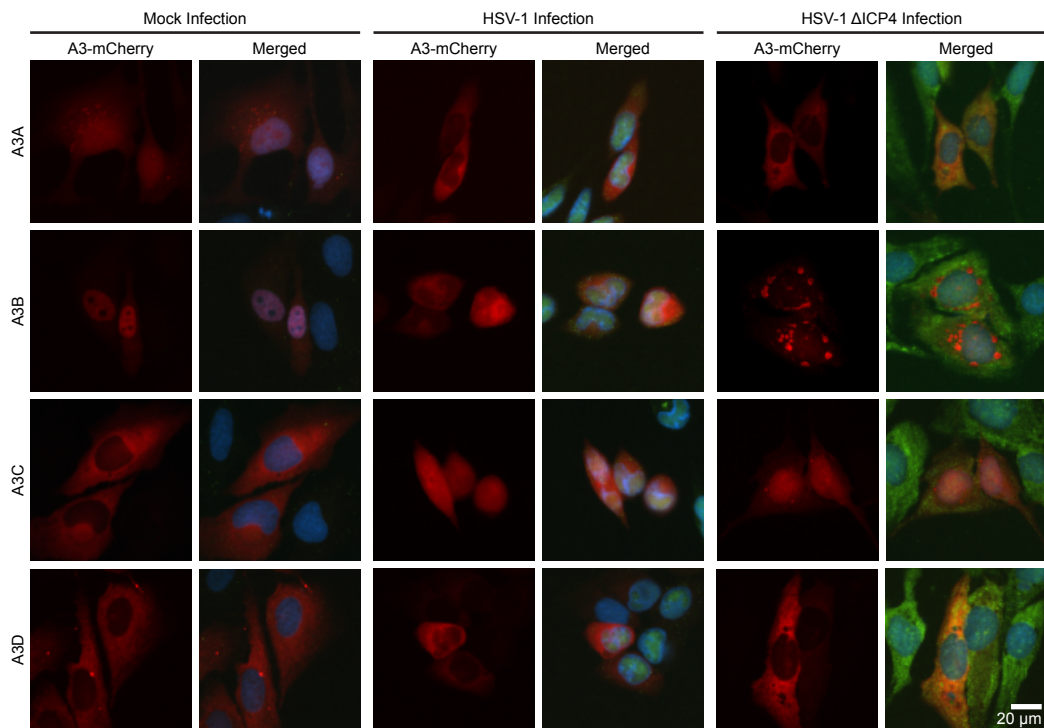
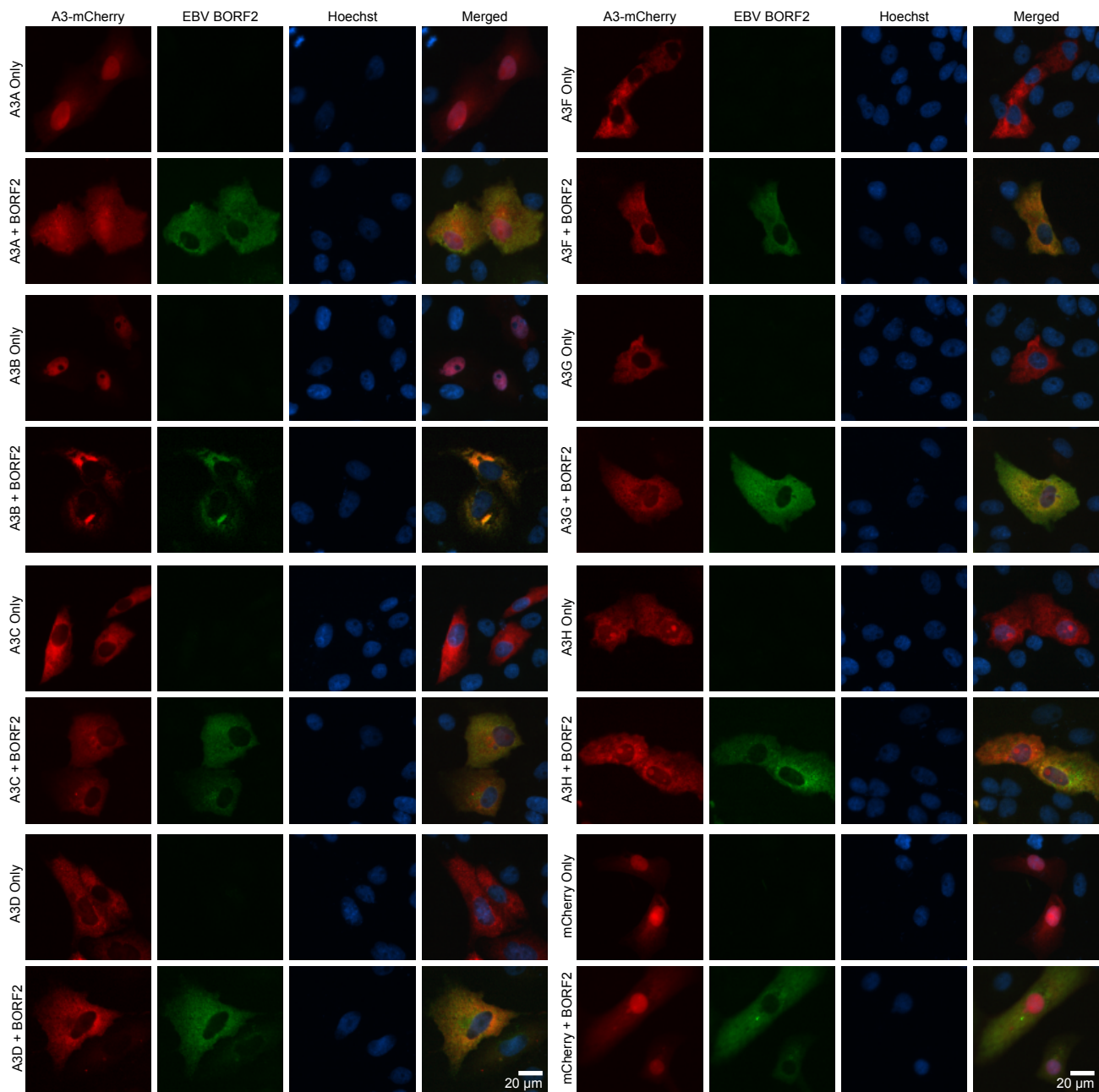
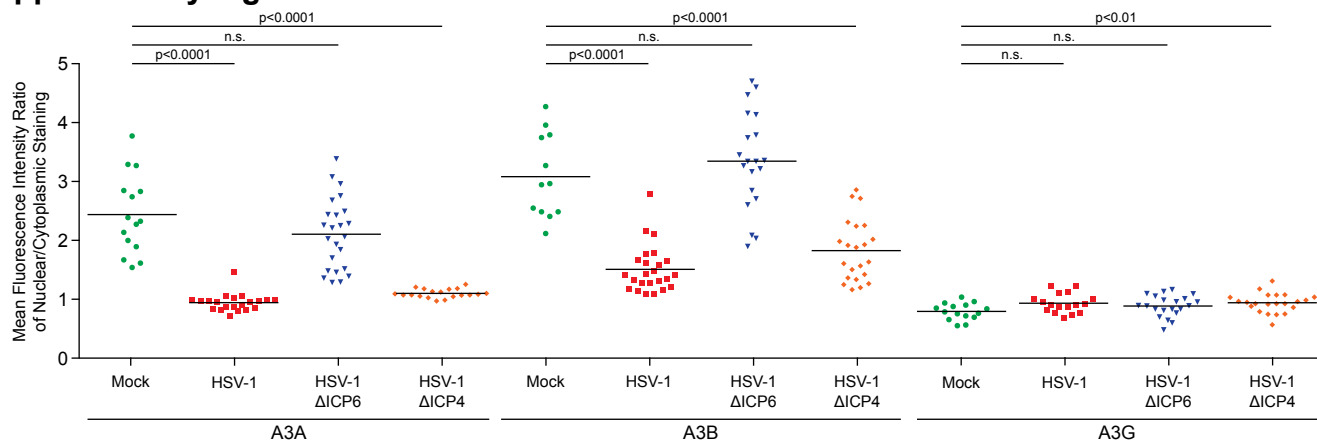
Fig 5

Fig 6**A****B**

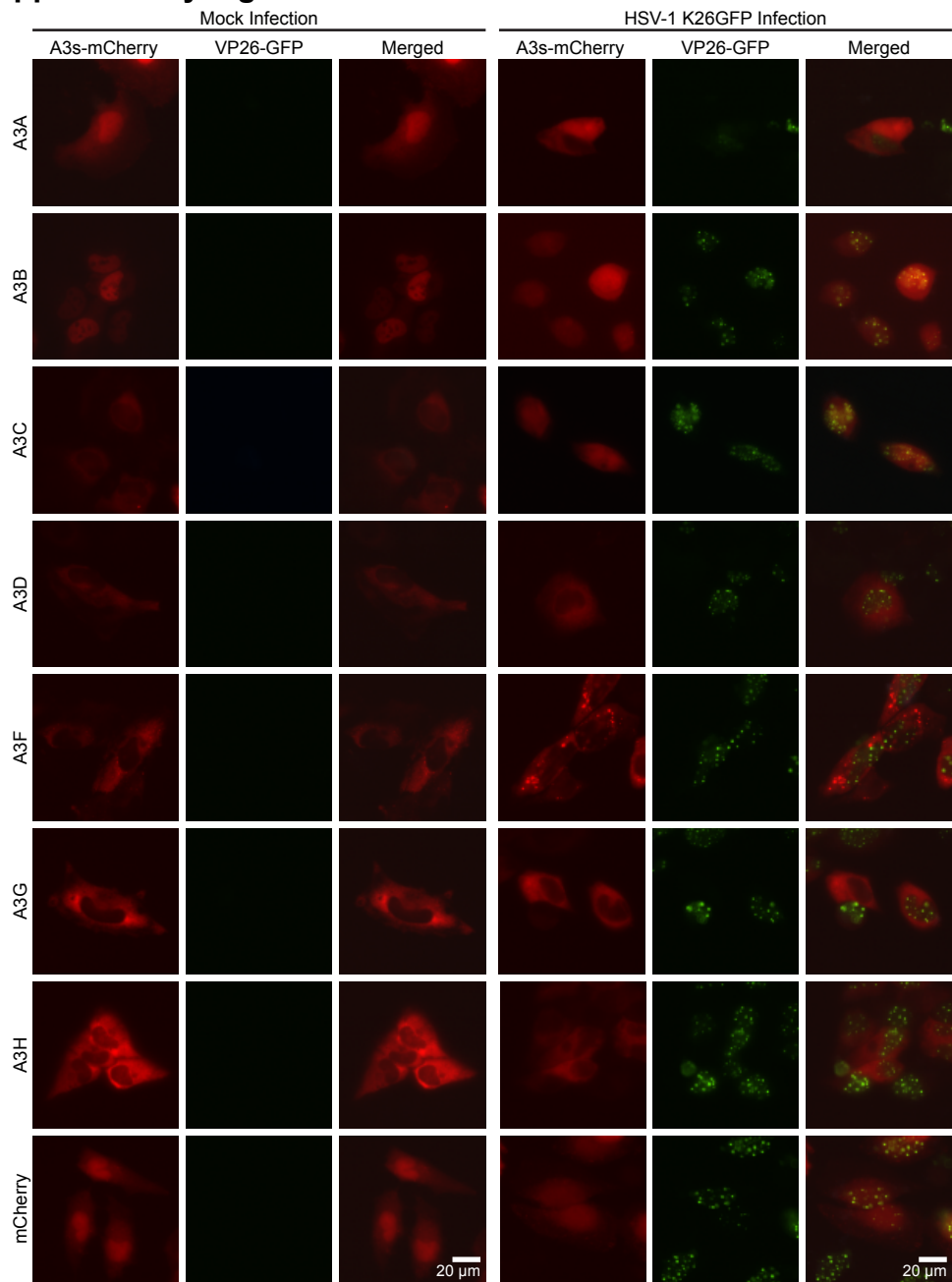
Supplementary Fig 1



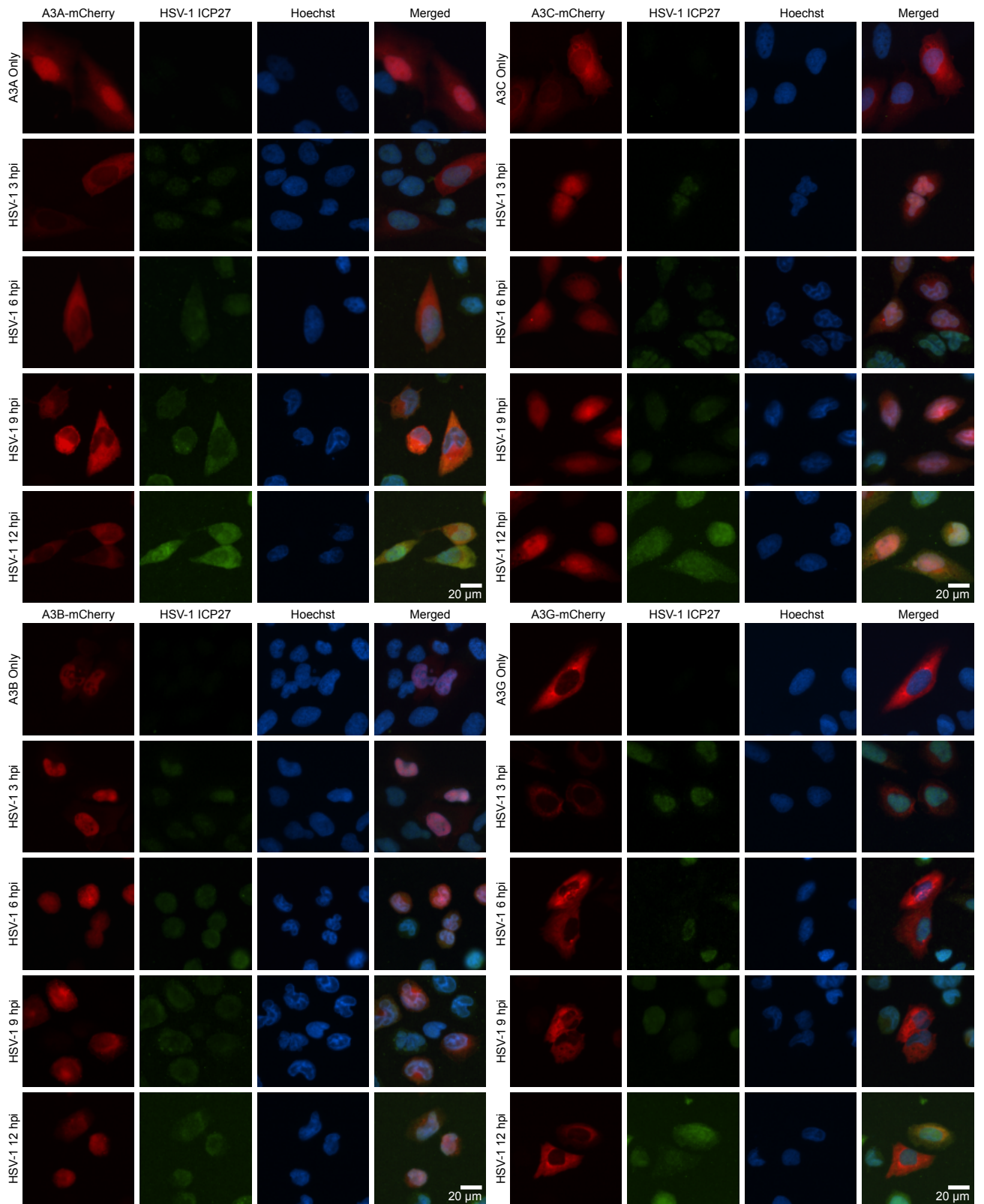
Supplementary Fig 2



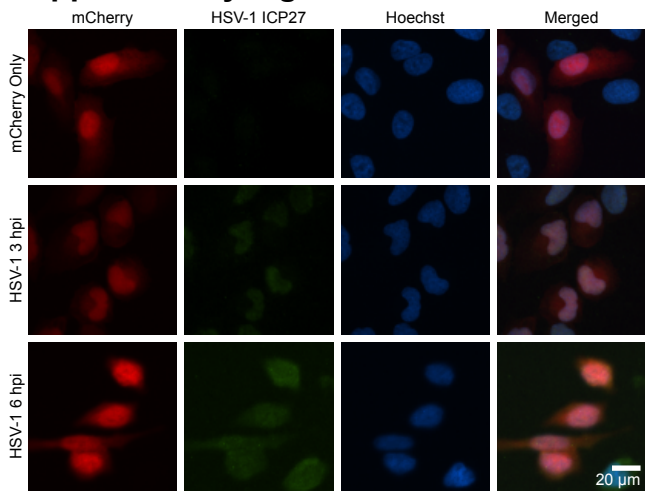
Supplementary Fig 3

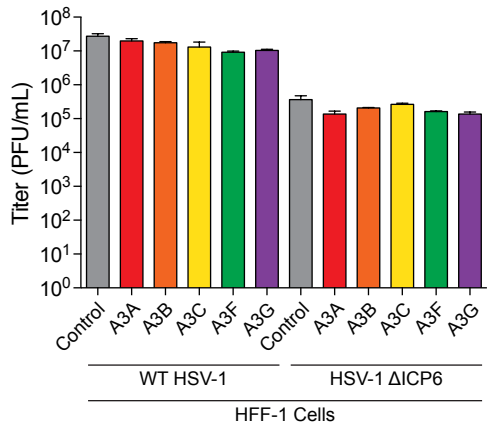


Supplementary Fig 4



Supplementary Fig 4



Supplementary Fig 5**A****B**